

Short Communication

Synthesis of Novel Fe-doped Amorphous TiO₂/C Nanofibers for Supercapacitors Applications

Gehan M. K. Tolba^{1,2}, Moaded Motlak^{2,3}, A. M. Bastaweesy¹, E. A. Ashour¹, Wael Abdelmoez¹, Mohamed El-Newehy^{4,5*}, and Nasser A. M. Barakat^{1,2,*}

¹Chemical Engineering Department, Faculty of Engineering, Minia University, El-Minia, Egypt

²BioNanosystem Department, Chonbuk National University, Jeonju 561-756, South Korea

³Department of Physics, College of Science, Anbar University, Anbar 31001, Iraq

⁴Petrochemical Research Chair, Department of Chemistry, College of Science, King Saud University, Riyadh 11451, Saudi Arabia

⁵Department of Chemistry, Faculty of science, Tanta University, Tanta 31527, Egypt

*E-mail: nasser@jbnu.ac.kr; melnewehy@ksu.edu.sa

Received: 5 November 2014 / Accepted: 11 January 2015 / Published: 24 February 2015

In this study, novel Fe-doped amorphous TiO₂/C nanofibers were successfully synthesized using a simple electrospinning technique. Typically, calcination of electrospun mats composed of titanium isopropoxide, iron acetate and polyvinylpyrrolidone (PVP) in argon atmosphere resulted in producing the introduced nanofibers. Scanning electronic microscopy (SEM), X-ray diffraction (XRD), transmission electron microscope (TEM), and X-ray photoelectron spectroscopy (XPS) were used for characterization of the produced nanofibers. The obtained nanofibers exhibit good electrochemical properties, presenting enhanced capacitive behavior with maximum specific capacitance of 137 F/g at a scan rate of 5mV/s in 1M KOH aqueous solution. The enhancement in the capacitance property of these materials could be attributed to the increased conductivity of TiO₂. Remarkably, it exhibits an excellent cycling stability.

Keywords: Amorphous titanium dioxide; Electrospinning; Supercapacitors; Specific capacitance

1. INTRODUCTION

Global rapid consumption of energy and environmental impact of traditional energy resources have inspired a growing need to develop new kinds of clean, sustainable energy conversion and storage systems such as batteries and super capacitors [1]. The super capacitors have a larger power density than common batteries and can be totally discharged without any deleterious. They can provide power pulses for a large variety of applications ranging from consumer electronics through hybrid

electric vehicles (HEVs) to industrial electric utilities. In addition, they are classified as an electrical double layer capacitor (EDLC) or a pseudo-capacitor depending on the charge-storage mechanism [2-4]. Moreover, their electrochemical performance depends on the electrode materials.

Such ideal materials are required to possess a high specific surface area, a controlled porosity, a high electronic conductivity, desirable electro active sites, and a high thermal and chemical stability[5]. For example, metal oxides nonomaterial are inexpensive and environmentally friendly with good electrochemical performance[6]. Amorphous TiO_2 (a- TiO_2) is one of the metal oxides that has got recent attention as an alternative to crystalline TiO_2 phases[7]. It has a bigger surface area leading to higher adsorptive, widely available in nature, can be prepared at room temperature, can be processed into different forms, and may allow much wider range of dopants. Studies showed that a- TiO_2 dye sensitized solar cell has been found to exhibits a higher efficiency as compared to the nano-crystalline TiO_2 layer[7, 8].

Nanoscale strongly enhances the physiochemical properties of the carbonaceous materials. Among the several reported nanostructures, one-dimensional structure meets the attention of the researchers due to the novel characteristics. Accordingly, much literature was introduced about 1D carbon, e.g. nanotube (CNT) and nanofibers (CNF). Among the 1D nanostructures, nanofibers have special interest. Owing to large surface-to-volume ratio, tunable transport properties, and unique surface chemistry, nanofibers are expecting to become important building blocks for harvesting solar, thermal, mechanical, and chemical energy, as well as electrical and electrochemical energy storage [9-14].

In this study, a- TiO_2 nanofibers doping with carbon and iron were prepared simply by electrospinning of a polymeric solution that contains titanium isopropoxide (TiIso) and iron acetate (FeAc) with polyvinylpyrrolidone (PVP). Then, calcination of the obtained nanofibers mats was conducted in argon gas at 900 °C for 3 hrs. The super capacitive properties of the produced material were investigated by using cyclic voltammetry in 1M KOH. The electrode is expected to give good super capacitive properties because it has a higher electrical conductivity and fibrous nature.

2. EXPERIMENTAL

2.1 Procedure

First, 1.8 g TiIso was added to a solution consisting of 3 g acetic acid and 2 g ethanol. The mixture was stirred for 15 min. Second, 20 g of 7.5% PVP were added to the prepared solution in order to prepare a TiIso and PVP sol-gel. Stirring continued until getting yellow transparent sol-gel. Third, 0.017g FeAc was dissolved in the minimum amounts of DMF and mixed with the original TiIso/PVP sol-gel. After that, the prepared sol-gels were subjected to electrospinning process. The solutions were briefly electro spun at 20 kV and a 15-cm working distance. Then, the formed nanofiber mats were initially dried for 24 h at 60 °C under vacuum and calcined. The calcination process was carried out under argon atmosphere at 1 atm and 900 °C for 3 h.

2.2 Characterization

Surface morphology was studied by scanning electron microscope (SEM, JEOL JSM-5900, Japan) and field-emission scanning electron microscope equipped with EDX analysis tool (FESEM, Hitachi S-7400, Japan). Information about the phase and crystallinity was obtained by using Rigaku X-ray diffractometer (XRD, Rigaku, Japan) with Cu K α ($\lambda = 1.540 \text{ \AA}$) radiation over Bragg angle ranging from 10 to 80°. Normal and high resolution images were obtained with transmission electron microscope (TEM, JEOL JEM-2010, Japan) operated at 200 kV equipped with EDX analysis. Electrochemical measurements were performed in a 1 M KOH solution using conventional three-electrode electrochemical cell. A Pt wire and an Ag/AgCl electrode were used as the auxiliary and reference electrodes, respectively.

3. RESULTS AND DISCUSSION

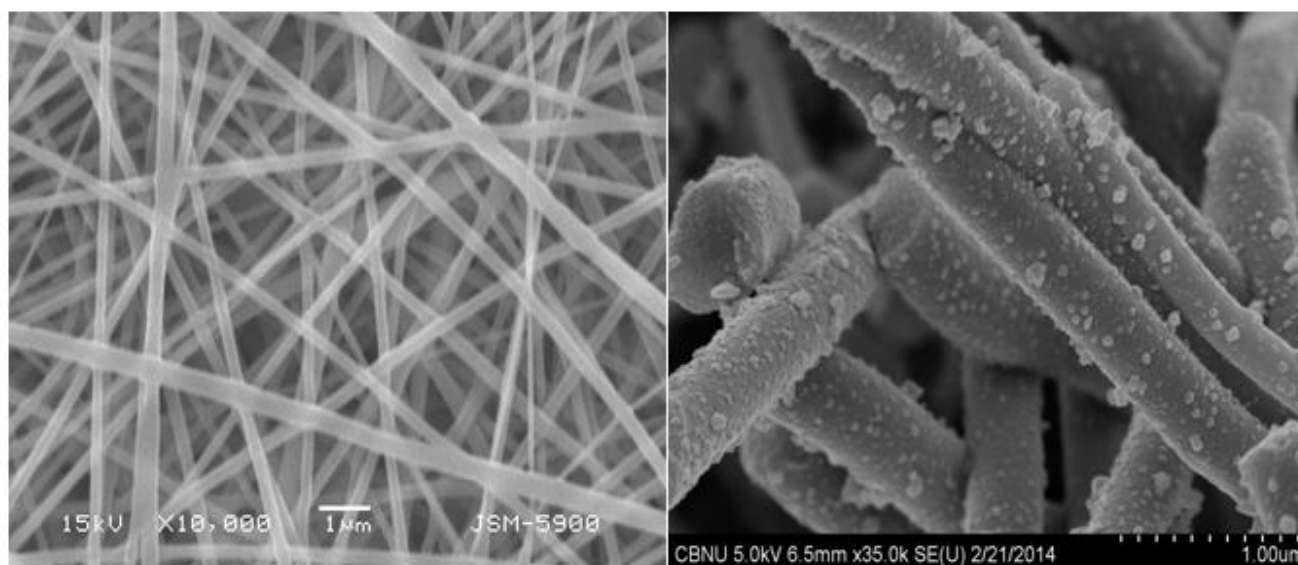


Figure 1. SEM image of the dried nanofibers (A), FESEM image of the nanofibers after calcination(B)

Fig.1 A shows SEM of the freshly prepared electrospun nanofiber mat. As shown in the figure, the nanofibers are clear and continuous without beads. In addition, they have a random distribution due to the bending instability accompanied with the spinning jet. Fig. 1B displays the FE SEM images of the obtained nanofibers after calcination. As displayed, the final product however exhibits a good morphology indicating that the calcination process did not affect the nanofibrous morphology. Calcination of the obtained electrospun nanofiber mats resulted in some decrease in the average diameter of the sintered nanofibers compared to the original ones. Moreover, the final nanofibers have a rough surface and irregular borders with an average diameter of 600 nm.

Structural characterization of the prepared nanofibers was studied and shown in Fig. 2A. The normal TEM image of the a-TiO₂ nanofibers shows a rough surface with irregular border. The inset in

Fig. 2A presents the SAED pattern where there are dislocation and imperfection. Typical XRD patterns of the nanofibers obtained after the calcination process are presented in Fig. 2B. No sharp diffraction peak of any crystalline phase is observed indicating that all the synthesized nanofibers have an amorphous structure except for a very broad peak in the range of 22–25° which corresponded to anatase phase.

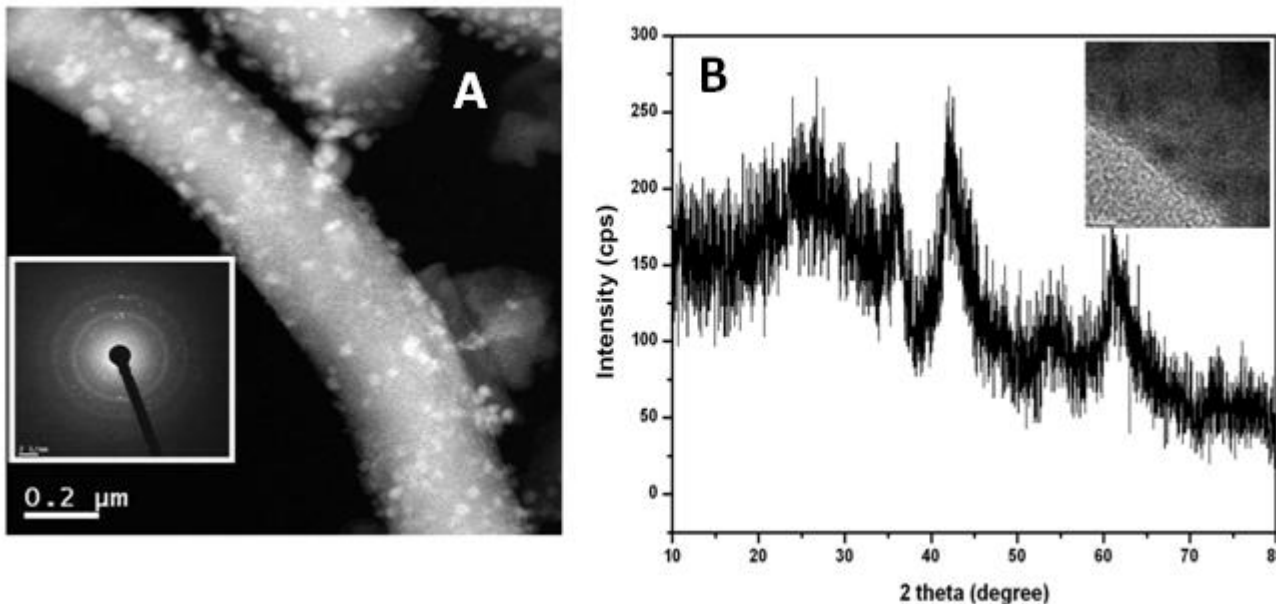


Figure 2. TEM images (A) (the inset displays SAED), and XRD pattern (B) (the inset displays HRTEM image) of the nanofibers.

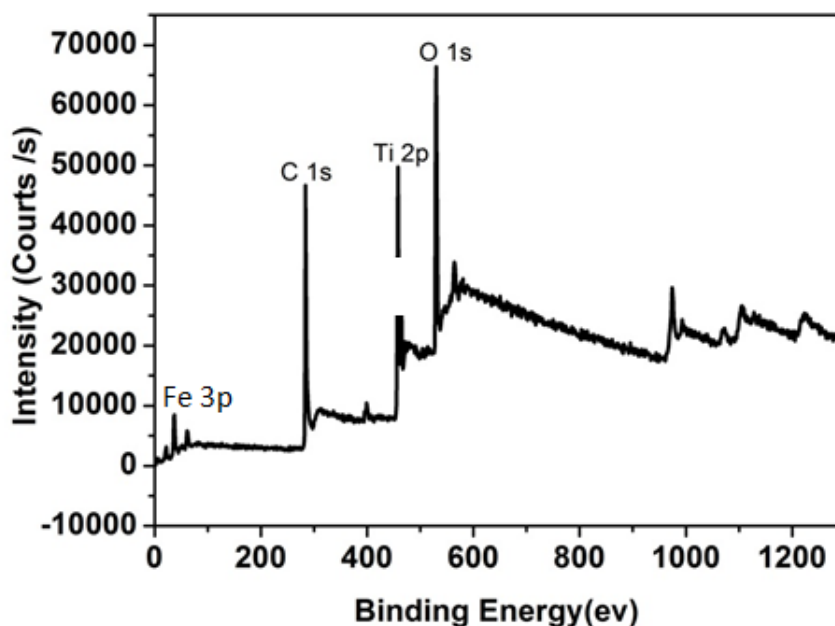


Figure 3. XPS spectrum of the obtained nanofibers.

In addition, a weak peak located at 2θ values of 62° was observed. The pattern indicates that the Fe species are highly dispersed in the TiO_2/C matrix without any crystalline formation. The presence of small diffractions around 62° might be due to the characteristic TiO_2 (anatase phase). These peaks are of low intensity due to the amorphous TiO_2 matrix. The HR TEM image (inset) of the part of the main TiO_2 NF indicates the absence of parallel atomic planes and reveals amorphous structure of the produced nanofibers. As displayed, dark portion from crystalline iron nano particles are presented along the nanofibers.

Surface composition and valence state of the prepared nanofibers were determined by X-ray photoelectron spectroscopy (XPS) analysis as shown in Fig. 3. As shown, the spectrum reveals the presence of $\text{Ti}2p$ (~ 464 eV) and (~ 459 eV) [15], $\text{C}1s$ (~ 285 eV) [15], $\text{Fe}3p$ (~ 62 eV), and $\text{O}1s$ (~ 530 eV) [16] core levels.

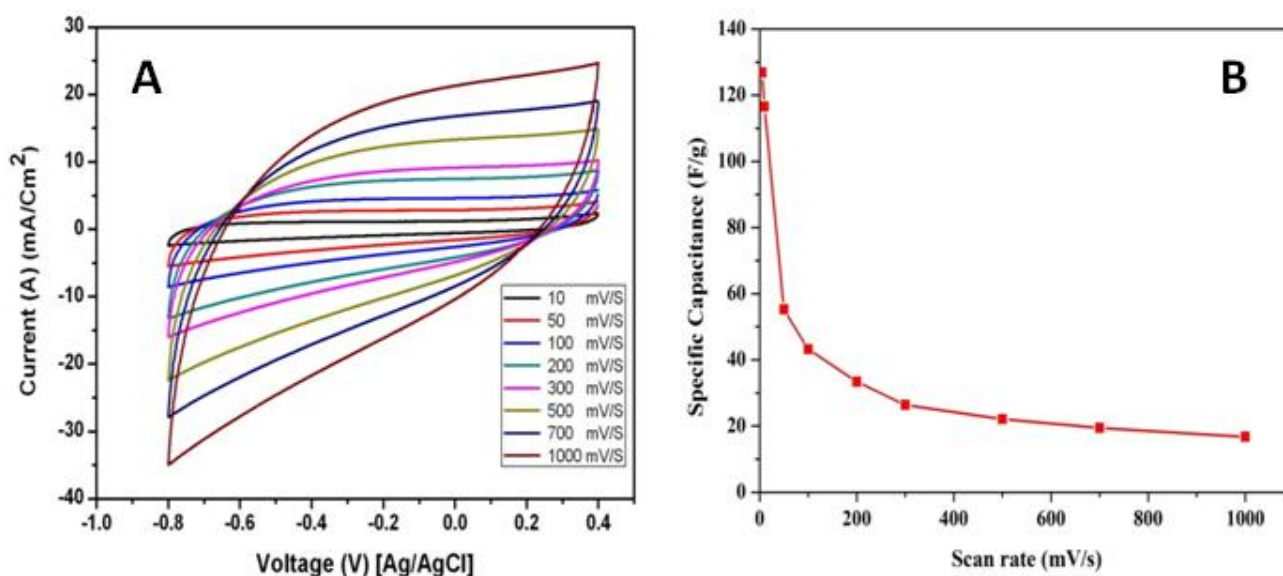


Figure 4. Cyclic voltammetry curves for the in 1 M KOH solution at different scan rates (A), and effect of the scan rate on the specific capacitance (B).

In this work, a nano scale amorphous TiO_2 electrode was chosen expecting an increase in the adsorptive capacity. It was reported that an increase in the concentration of interfacial regions in amorphous materials may form percolation pathways to facilitate the diffusion of ions [17]. Moreover, the carbon has a very good electrical conductivity, thus it exhibits much lower resistance for the electron transfer. Therefore, the presence of Fe and C was means an increase in the conductivity of the TiO_2 support. Fig. 4A displays the CV curves of the introduced nanofibers electrode at different scan rates. All the CV curves exhibits an almost rectangular shape without any obvious redox peaks or Faradic reactions indicating good charge propagation within the electrodes and therefore, a good capacitive behavior. Additionally, they reveal that the mechanism of electrochemical storage is typical for electrochemical double layer capacitors. According to this theory, energy storage in these electrodes is the accumulation of ionic charge in the double layer at the electrode/electrolyte interface and this might due to the high surface area. The relatively linear increase of the current density with

increasing scan rate demonstrates that the charge is primarily non-faradic in nature and the contribution of the faradic part might be very little, if it exists at all. Moreover, The CV measurements indicate that the introduced nanofibers were stable in the 1M KOH electrolyte within the potential range of interest. This suggests that nanofibers were appropriate electrode materials for electrochemical super capacitors. Furthermore, the nano fibers exhibit the specific capacitance of 137 F/g at a scan rate of 5 mV/s.

The effect of different scan rates on the capacitive behavior of electrode was studied and the results are presented in Fig. 4B. As expected, the specific capacitance decreased gradually as the scan rate increases. That may be due to that too large currents may reduce the accessibility of ions through the micro pores and thus reduces the specific capacitance indicating not only a reduction in the equivalent series resistance of the nanofibers web electrode, but also a reduction in the ability of ions to penetrate the pores.

4. CONCLUSION

Amorphous titanium oxide doping with iron and carbon nanofibers can be synthesized by the electrospinning of a sol-gel composed of titanium isopropoxide, iron acetate and polyvinylpyrrolidone (PVP) followed by calcinations process. The modified amorphous titanium oxide nanofibers can be exploited as potential electrode material for the electrochemical supercapacitors. The improved electrochemical performance of the electrode was attributed mainly to the high specific surface area, fast electron transport, and increasing in the conductivity of the TiO₂.

ACKNOWLEDGEMENT

This project was supported by NSTIP strategic technologies programs, number (11-ENE 1917-02) in the Kingdom of Saudi Arabia.

References

1. T. Chen, L. Dai, *Materials Today* 16 (2013) 272-280.
2. Y. Cai, Y. Wang, S. Deng, G. Chen, Q. Li, B. Han, R. Han, Y. Wang, *Ceramics International* 40 (2014) 4109-4116.
3. J. Xiao, L. Wan, S. Yang, F. Xiao, S. Wang, *Nano letters* 14 (2014) 831-838.
4. W. Chen, C. Xia, H.N. Alshareef, *ACS nano* 8 (2014) 9531-9541.
5. K.H. An, W.S. Kim, Y.S. Park, J.-M. Moon, D.J. Bae, S.C. Lim, Y.S. Lee, Y.H. Lee, *Advanced Functional Materials* 11 (2001) 387-392.
6. C. Yuan, X. Zhang, L. Su, B. Gao, L. Shen, *Journal of Materials Chemistry* 19 (2009) 5772-5777.
7. H. Xiong, M.D. Slater, M. Balasubramanian, C.S. Johnson, T. Rajh, *The Journal of Physical Chemistry Letters* 2 (2011) 2560-2565.
8. J. Hensel, G. Wang, Y. Li, J.Z. Zhang, *Nano letters* 10 (2010) 478-483.
9. N.A.M. Barakat, M.F. Abadir, K.T. Nam, A.M. Hamza, S.S. Al-Deyab, W.-i. Baek, H.Y. Kim, *J. Mater. Chem.* 21 (2011) 10957-10964.

10. N.A.M. Barakat, K.A. Khalil, I.H. Mahmoud, M.A. Kanjwal, F.A. Sheikh, H.Y. Kim, *J. Phys. Chem. C* 114 (2010) 15589-15593.
11. N.A.M. Barakat, B. Kim, H.Y. Kim, *J. Phys. Chem. C* 113 (2008) 531-536.
12. N.A.M. Barakat, B. Kim, S.J. Park, Y. Jo, M.-H. Jung, H.Y. Kim, *J. Mater. Chem.* 19 (2009) 7371-7378.
13. N.A.M. Barakat, B. Kim, C. Yi, Y. Jo, M.-H. Jung, K.H. Chu, H.Y. Kim, *J. Phys. Chem. C* 113 (2009) 19452-19457.
14. H. Wu, R. Zhang, X. Liu, D. Lin, W. Pan, *Chem. Mater.* 19 (2007) 3506-3511.
15. H. Kamisaka, T. Adachi, K. Yamashita, *The Journal of chemical physics* 123 (2005) 084704.
16. N. McIntyre, D. Zetaruk, *Analytical Chemistry* 49 (1977) 1521-1529.
17. K. Kaur, C.V. Singh, *Energy Procedia* 29 (2012) 291-299.

© 2015 The Authors. Published by ESG (www.electrochemsci.org). This article is an open access article distributed under the terms and conditions of the Creative Commons Attribution license (<http://creativecommons.org/licenses/by/4.0/>).